Sedimentary record of marine and terrigenous organic matter delivery to the Shatsky Rise, western North Pacific, over the last 130 kyr

Miki Amo*, Masao Minagawa

Graduate School of Environmental Earth Science, Hokkaido University, Sapporo 060-0810, Japan

Abstract

Biomarker and carbon isotopic analyses of piston core samples were undertaken to reconstruct changes over the last 130 kyr in the delivery of organic matter from marine plankton and terrestrial sources to sediments on the Shatsky Rise in the western North Pacific. Marine and terrigenous organic matter delivery was reconstructed from alkenone and *n*-alkane concentrations using multiple regression analysis, which gave results consistent with a $\delta^{13}C$ mass balance model. Marine organic carbon comprises more than 86% of the total organic carbon throughout the sediment record. Fluxes of marine organic carbon were higher in glacial times, indicating that marine production increased in these periods. We conclude that in addition to the southward shift of the Subarctic front, eolian dust supply at this location played an essential role in enhancing paleoproduction during the last glacial maximum.
© 2003 Elsevier Ltd. All rights reserved.

1. Introduction

The flux of organic carbon in marine sediments has been used to estimate carbon budgets in the past as climate has changed. The total organic carbon (TOC) content in sediment and the concentration of key biomarker molecules have been used as clues to estimate marine productivity (e.g., Sarnthein et al., 1988; Sicre et al., 2000). Biomarkers that originate from marine plankton and terrestrial higher plants are recognized as proxies of organic matter delivery to marine environments (Jasper and Gagosian, 1993; Villanueva et al., 1997). Long chain alkenones (LCA) are biosynthesized by some haptophyte algae (Volkman et al., 1980; Marlowe et al., 1984). Hence, LCA concentration in marine sediment can be used to reconstruct haptophyte paleoproductivity (Rostek et al., 1997; Villanueva et al., 1998). The odd-numbered long chain *n*-alkanes originate from epicuticular wax in higher plants (Eglinton

and Hamilton, 1967) and are useful for identifying typical terrestrial plants. The long chain *n*-alkanes in pelagic sediments are derived from land by eolian transport (Simoneit, 1977; Gagosian and Peltzer, 1986).

In the middle latitudes of the western North Pacific, Kawahata et al. (1999) first estimated primary productivity based on TOC and reconstructed temporal changes of productivity during the last 300 kyr in core S2612 (32°20′N, 157°51′E) from the Shatsky Rise. Maeda et al. (2002) further reported changes in productivity during the last 180 kyr based on the northern site core NGC108 (36°37′N, 158°21′E). They assumed that all organic carbon originated from in situ marine plankton, on the basis of the C/N elemental ratios of sediments, and argued that latitudinal shift of oceanic fronts in glacial periods increased biological productivity.

While it is accepted that TOC in pelagic sediments is largely of marine planktonic origin, it has also been reported that in the eastern tropical Pacific up to 20% of the TOC could be supplied by eolian transport of terrestrial organic matter (Prahl et al., 1989). The western North Pacific is a region where terrestrial dust is continuously transported by the monsoon wind system

---

* Corresponding author. Fax.: +81-11-706-4867.
  E-mail address: amou@ees.hokudai.ac.jp (M. Amo).

(Duce et al., 1991), and the strength of such transport is likely enhanced in glacial periods. The dust flux at the Shatsky Rise was higher in glacial periods than interglacial periods (Hovan and Rea, 1991; Maeda et al., 2002). Increased dust flux in glacial times was also reported at the Hess Rise, to the east of the Shatsky Rise (Kawahata et al., 2000). Based on these findings, it is worthwhile checking whether sedimentary TOC might contain a significant proportion of terrigenous organic carbon, especially in the most recent ice age.

To estimate marine and terrigenous organic carbon flux in the middle latitudes of the western North Pacific, we analyzed alkenones and *n*-alkanes, as well as TOC and $\delta^{13}C$, in a piston core from the Shatsky Rise, which recovered sediment that has accumulated over the last 130 kyr. We report here the interrelation between paleoproductivity and sea surface temperature as indicated by $U_{37}^{K'}$, and we also consider the latitudinal shift of the Subarctic front and the role of terrestrial dust supply to this region.

2. Materials and methods

2.1. Samples

Piston core S-2 (core length: 802 cm) and multiple core AC-2 (core length: 30 cm) were independently collected in 1996 from the same site (33°21.8′N, 159°07.7′E, water depth: 3107 m) on the Shatsky Rise (Fig. 1) during cruise KH96-3 of the R/V Hakuho Maru. Sediment was sampled in stainless-steel tubes (12×2×2 cm) for organic matter analyses. Samples were kept in a freezer at −20 °C; 2-cm-thick sub-samples were taken in the laboratory for biomarker analysis and for bulk organic matter analysis.

The sediment chronology was established by Yamane (2003), according to the conventional procedure of comparing the $\delta^{18}O$ values of the planktonic foraminifera *Globorotalia inflata* relative to the SPECMAP $\delta^{18}O$ curve (Fig. 2a). The estimated ages are listed in Table 1, and the detailed age model will be published elsewhere (Yamane, 2003). Because the top of the piston core was lost in the operation, we used the multiple core from the same site to splice together a continuous sediment record, after carefully adjusting the two chronostratigraphies using the $\delta^{18}O$ profile. Sedimentation rate is based on the $\delta^{18}O$ stratigraphy (Table 1 and Fig. 2b).

2.2. Bulk analysis

Each sediment sample was dried at 60 °C in an electric oven and was then decarbonated by 1 molar HCl, rinsed with distilled water to remove salt components, and then dried again. The carbon content and carbon isotopic ratio of organic matter were determined by the flow-injection method using a Finnigan MAT 252 mass spectrometer connected with a Fisons NA1500 elemental analyzer. The amount of carbon was then converted to the concentration on a bulk dry sediment basis. The isotope results are presented using the conventional delta notation and are calibrated to PDB standards. The analytical error was estimated to be within 0.2‰ based on replicate runs of an amino acid reagent.

2.3. Lipid analysis

The lipid fraction in each sediment sample was extracted sequentially with methanol, chloroform/methanol (1:1), chloroform/methanol (3:1), and chloroform, using an ultrasonicator (20 min). An internal standard mixture was added to wet sediment samples (5–15 g) prior to extraction. The lipid fractions were washed with distilled water to remove non-lipid components and sea salts, and then dried over Na_2SO_4. The lipid extract was saponified with 1 molar KOH (95% methanol/5% water) and added distilled water. The neutral fraction was extracted with *n*-hexane/diethyl ether (9:1) and *n*-hexane/diethyl ether (1:1), and was divided into following three fractions by column chromatography (Merck silica gel 60, 70–230 mesh ASTM). The *n*-alkanes (F1), ketones (F2) and *n*-alcohols (F3) were eluted with hexane, dichloromethane and chloroform, respectively.

F1 and F2 were analyzed quantitatively using a Hewlett Packard 6890 series gas chromatograph (GC) equipped with a splitless injector, a fused-silica capillary column DB-5 (length, 30 m; i.d., 0.32 mm; thickness, 0.25 μm) and a flame ionization detector. Helium was used as the carrier gas. The oven temperature for F1 analysis was programmed from 50 to 150 °C at 20 °C/min, from 150 to 320 °C at 5 °C/min, and then held at 320 °C for 20 min. Peak identification of F1 was performed by the gas chromatographic retention time of each peak compared to those of authentic standards. Internal standard (*n*-$C_{24}D_{50}$ alkane) recoveries were above 86% in every sample. Replicate analysis (nine times) of a single sediment sample showed that the analytical error in the procedures was less than 6% of the concentration of the C_{23}–C_{33} *n*-alkanes.

The oven temperature program of F2 analysis was from 50 to 180 °C at 20 °C/min, from 180 to 320 °C at 3 °C/min, and then held at 320 °C for 20 min. The compounds in F2 were identified by mass spectral analysis using a Hewlett Packard 5973 gas chromatograph-mass selective detector. Internal standard (18-Pentatriacontanone) recoveries of this fraction were more than 80% in every sample. Replicated analyses (four times) of a sediment showed that the analytical error in the procedures was less than 3% of the concentration for C_{37} alkenones and the standard deviation was 0.006 for $U_{37}^{K'}$.
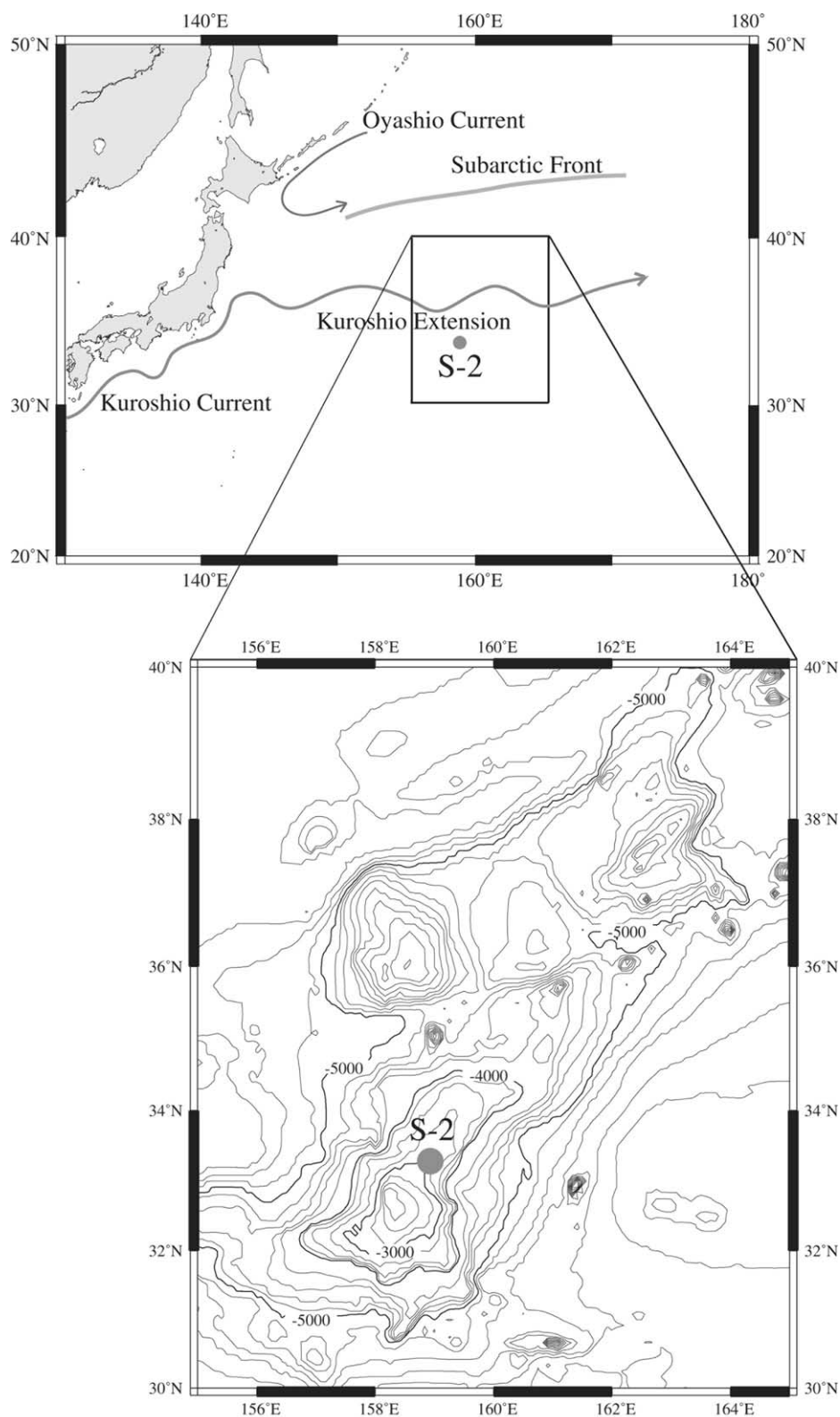
Fig. 1. Map showing present current system and location of the core analyzed in this study.
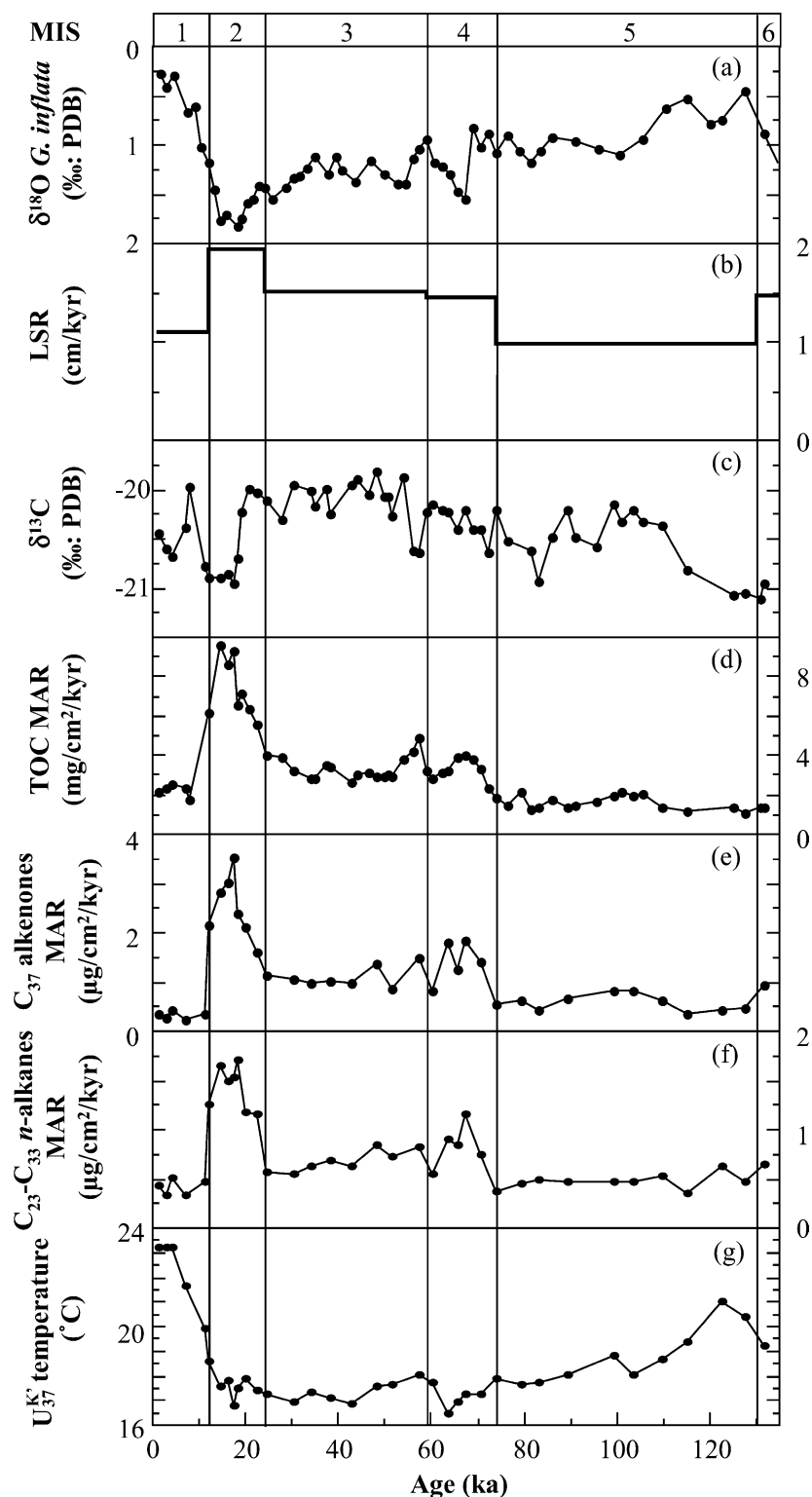
Fig. 2. Isotopic and biomarker profiles plotted against age in core S-2 and AC-2 over the last 130 kyr: (a) $\delta^{18}O$ of *G. inflata*. (Yamane, 2003); (b) linear sedimentation rate (LSR); (c) $\delta^{13}C$ of TOC; (d) TOC mass accumulation rate (MAR); (e) C_{37} alkenones MAR; (f) C_{23}–C_{33} *n*-alkanes MAR; (g) $U^{K'}_{37}$ temperature.

Table 1
Core depth (Depth), calendar age (Age), linear sedimentation rate (LSR), dry bulk density (DBD), total organic carbon (TOC) content, $\delta^{13}C$ of TOC, C_{37} alkenones concentration, C_{23}–C_{33} n-alkanes concentration, the carbon preference index (CPI) of n-alkanes, $U_{37}^{K'}$ and SST estimated from $U_{37}^{K'}$ values in the S-2 and AC-2 sediments

Depth (cm)	Age (ka)	LSR (cm/kyr)	DBD (g/cm³)	TOC (%)	$\delta^{13}C$ (‰)	C_{37} alkenone (µg/g)	C_{23}–C_{33} n-alkane (µg/g)	CPI	$U_{37}^{K'}$	SST (°C)
1.0[a]	1.4	1.1	0.72	0.28	−20.4	0.47	0.54	2.6	0.83	23.2
3.0[a]	2.8	1.1	0.70	0.31	−20.6	0.36	0.43	2.6	0.83	23.2
5.0[a]	4.2	1.1	0.85	0.27	−20.7	0.48	0.56	4.9	0.83	23.2
9.0[a]	6.9	1.1	0.90	0.24	−20.4	0.26	0.35	5.5	0.77	21.6
10.5[a]	7.9	1.1	0.90	0.18	−20.0	–	–	–	–	–
15.0[a]	11.0	1.1	0.94	–	−20.8	0.33	0.46	3.2	0.72	19.9
13.0	12.1	1.9	1.00	0.32	−20.9	1.11	0.65	4.1	0.67	18.6
18.0	14.7	1.9	0.91	0.55	−20.9	1.61	0.94	5.3	0.64	17.6
21.0	16.2	1.9	0.88	0.51	−20.9	1.76	0.88	4.9	0.65	17.8
23.0	17.3	1.9	0.93	0.52	−20.9	1.95	0.85	4.3	0.61	16.8
25.0	18.3	1.9	0.90	0.38	−20.7	1.37	0.98	4.5	0.63	17.5
26.7	19.2	1.9	0.90	0.41	−20.2	–	–	–	–	–
28.0	19.9	1.9	0.85	–	–	1.29	0.72	4.6	0.65	17.9
30.0	20.9	1.9	0.85	0.38	−20.0	–	–	–	–	–
33.0	22.4	1.9	0.98	0.30	−20.0	0.86	0.61	4.9	0.63	17.4
37.0	24.5	1.5	0.90	0.29	−20.1	0.84	0.42	5.4	0.63	17.3
42.0	27.9	1.5	0.87	0.30	−20.3	–	–	–	–	–
45.6	30.3	1.5	0.87	0.25	−20.0	0.79	0.42	4.1	0.62	17.0
51.0	34.0	1.5	0.98	0.19	−20.0	0.67	0.42	5.4	0.63	17.3
52.6	35.1	1.5	0.98	0.19	−20.2	–	–	–	–	–
56.0	37.3	1.5	0.97	0.24	−20.0	–	–	–	–	–
57.3	38.2	1.5	0.97	0.24	−20.2	0.70	0.47	5.3	0.62	17.1
64.3	42.9	1.5	1.03	0.17	−19.9	0.61	0.41	5.3	0.61	16.9
65.8	43.9	1.5	1.07	0.19	−19.9	–	–	–	–	–
69.6	46.5	1.5	1.07	0.20	−20.0	–	–	–	–	–
71.8	48.0	1.5	1.08	0.18	−19.8	0.84	0.52	5.0	0.64	17.6
74.4	49.7	1.5	1.08	0.18	−20.1	–	–	–	–	–
75.8	50.7	1.5	1.09	0.18	−20.1	–	–	–	–	–
76.9	51.4	1.5	1.09	0.18	−20.3	0.55	0.44	6.1	0.64	17.6
80.8	54.1	1.5	1.04	0.24	−19.9	–	–	–	–	–
84.1	56.3	1.5	1.04	0.27	−20.6	–	–	–	–	–
85.8	57.4	1.5	1.02	0.32	−20.6	0.98	0.54	5.8	0.65	18.0
88.9	59.0	1.4	1.02	0.22	−20.2	–	–	–	–	–
90.8	60.3	1.4	1.05	0.19	−20.2	0.53	0.36	5.3	0.64	17.7
93.7	62.3	1.4	1.05	0.21	−20.2	–	–	–	–	–
95.8	63.7	1.4	1.09	0.20	−20.2	1.15	0.57	5.4	0.60	16.5
98.5	65.6	1.4	1.09	0.25	−20.4	0.81	0.54	5.9	0.62	16.9
100.8	67.2	1.4	1.07	0.26	−20.2	1.18	0.75	5.0	0.63	17.3
103.3	68.9	1.4	1.07	0.24	−20.4	–	–	–	–	–
105.8	70.6	1.4	1.08	0.22	−20.4	0.91	0.48	5.9	0.63	17.3
108.2	72.3	1.4	1.08	0.15	−20.6	–	–	–	–	–
110.8	74.1	1.0	1.12	0.17	−20.2	0.51	0.34	5.4	0.65	17.9
113.0	76.4	1.0	1.12	0.13	−20.5	–	–	–	–	–
115.8	79.2	1.0	1.14	0.19	–	0.57	0.40	6.0	0.64	17.6
117.8	81.2	1.0	1.14	0.12	−20.6	–	–	–	–	–
119.8	83.2	1.0	1.09	0.13	−20.9	0.40	0.45	5.2	0.64	17.7
122.6	86.1	1.0	1.09	0.16	−20.5	–	–	–	–	–
125.8	89.3	1.0	1.06	0.13	−20.2	0.64	0.45	5.7	0.65	18.0
127.4	90.9	1.0	1.06	0.14	−20.5	–	–	–	–	–
131.8	95.4	1.0	1.03	0.16	−20.6	–	–	–	–	–
135.8	99.4	1.0	1.05	0.19	−20.2	0.80	0.46	6.0	0.68	18.8

Table 1 (*continued*)

Depth (cm)	Age (ka)	LSR (cm/kyr)	DBD (g/cm³)	TOC (%)	δ¹³C (‰)	C₃₇ alkenone (μg/g)	C₂₃–C₃₃ n-alkane (μg/g)	CPI	U^K'_{37}	SST (°C)
137.3	100.9	1.0	1.05	0.21	−20.3	–	–	–	–	–
139.8	103.4	1.0	1.05	0.19	−20.2	0.80	0.46	5.0	0.65	18.1
141.9	105.6	1.0	1.05	0.20	−20.3	–	–	–	–	–
145.8	109.5	1.0	1.08	0.13	−20.4	0.58	0.50	5.4	0.67	18.7
151.5	115.3	1.0	1.08	0.11	−20.8	0.34	0.33	6.4	0.70	19.4
158.5	122.3	1.0	1.09	–	–	0.42	0.58	2.8	0.75	21.0
161.0	124.9	1.0	1.09	0.13	−21.1	–	–	–	–	–
163.5	127.4	1.0	1.04	0.10	−21.1	0.45	0.45	5.6	0.73	20.4
167.5	131.0	1.5	1.04	0.09	−21.1	–	–	–	–	–
168.5	131.6	1.5	0.96	0.10	−21.0	0.67	0.47	5.3	0.69	19.2

[a] AC-2.

Paleo-SST estimates were then calculated from individual alkenone concentrations using the equation established by Prahl et al. (1988):

$$T \ (^\circ C) = \frac{U^{K'}_{37} - 0.039}{0.034} \qquad (1)$$

3. Results

3.1. TOC and carbon isotopic compositions

TOC concentrations in the whole core range from 0.09 to 0.55%, with an average of 0.23% (Table 1). TOC is highest in the 12–20 ka interval, which is consistent with the results of the Shatsky Rise core S2612 (32°N) reported by Kawahata et al. (1999).

Organic δ¹³C values range from −21.1 to −19.8‰, and average −20.4‰ (Table 1). Because the δ¹³C of marine organic matter is around −20‰ in middle latitudes (Goericke and Fry, 1994), these results suggest that the TOC in Shatsky Rise sediments is mostly marine organic matter. However, some negative values were found in the late period of marine isotope stage (MIS) 2 and the early part of MIS 5 (Fig. 2c), indicating that some events did cause carbon isotopic shifts.

3.2. Biomarkers

Concentrations of C₃₇ alkenones range from 0.26 to 1.95 μg/gdw (per g dry bulk weight) with an average of 0.79 μg/gdw (Table 1). Concentrations of C₂₃–C₃₃ n-alkanes range from 0.33 to 0.98 μg/gdw with an average of 0.55 μg/gdw (Table 1). Molecular distributions of C₂₃–C₃₃ n-alkanes show odd to even carbon number predominance. A typical pattern at the last glacial maximum (LGM) is shown in Fig. 3. The distribution of n-alkanes shows n-C₃₁ predominance in the whole core—C₃₁/(C₂₇ + C₂₉ + C₃₁) > 40%. Carbon preference index (CPI) is defined as the ratio of odd carbon number n-alkanes to

even n-alkanes (Bray and Evans, 1961). CPI values of n-alkanes vary from 2.6 to 6.4, with an average of 5.0 excluding two samples near the core top (Table 1). These values suggest that most of the n-alkanes in this core originate from higher plant waxes (Collister et al., 1994). The temporal variation of the C₂₃–C₃₃ n-alkanes concentrations was in agreement with those of other terrestrial components concentrations such as Al and Ti (Murayama et al., 1998). These results suggest that the C₂₃–C₃₃ n-alkanes in most samples could be mainly terrestrial origin.

3.3. Mass accumulation rate of organic components

To quantify the variability of the sediment flux for each component, we determine the mass accumulation rate (MAR) using the following formula:
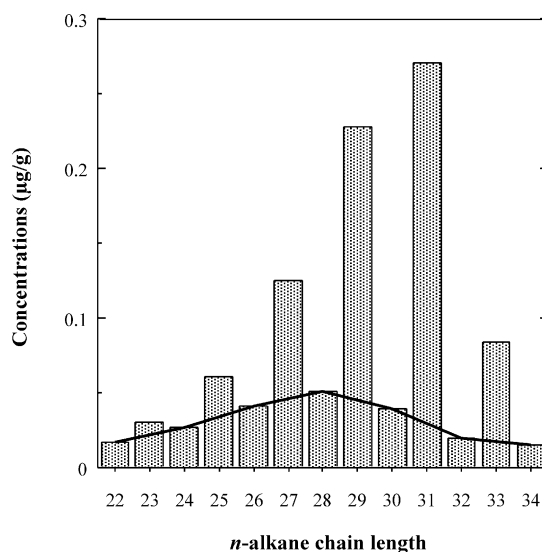

Fig. 3. The distributions of n-alkane chain length (18.3 ka). The odd C₂₃–C₃₃ n-alkanes correspond to the area situated above the line.

$$MAR = CC \times LSR \times DBD \qquad (2)$$

where CC, LSR and DBD are the concentration of the compound, the linear sedimentation rate (cm/kyr) and the dry bulk density (g/cm^3), respectively. LSR, DBD and MAR of organic components are shown in Table 1 and Fig. 2. TOC MAR ranges from 1.1 to 9.6 mg/cm^2/kyr, with an average of 3.3 mg/cm^2/kyr for the whole core (Fig. 2d). TOC MAR is highest during MIS 2 and noticeably lower during MIS 1 and 5. C_{37} alkenones MAR ranges from 0.28 to 3.52 μg/cm^2/kyr, with an average of 1.17 μg/cm^2/kyr for the whole core (Fig. 2e). C_{23}–C_{33} *n*-alkanes MAR ranges from 0.33 to 1.70 μg/cm^2/kyr, with an average of 0.75 μg/cm^2/kyr for the whole core (Fig. 2f). C_{37} alkenones MAR and C_{23}–C_{33} *n*-alkanes MAR vary in parallel with glacial/interglacial changes. Moreover, TOC MAR, C_{37} alkenones MAR and C_{23}–C_{33} *n*-alkanes MAR show similar variation patterns with the highest values in glacial stage 2 and lower values in interglacial stages.

3.4. $U_{37}^{K'}$-derived temperature

The alkenone unsaturation index was used to estimate surface water temperature for 36 samples. Generally, temperature estimates from $U_{37}^{K'}$ have used the equation proposed by Prahl et al. (1988), which was based on *Emiliania huxleyi* culture experiments. In the western North Pacific, a sediment trap experiment was carried out at a nearby location (34°25′N, 177°44′W) in the NOPACCS project. A preliminary microbiology study has determined that *E. huxleyi* is the dominant species and comprises more than 70% of the total coccolith flux. *Gephyrocapsa oceanica* and *Gephyrocapsa mullerae*, other alkenone producers, contribute less than 2% to total coccolith flux (Tanaka, personal communication). We assumed that this would apply during the entire period of this core, and therefore we adopted the Prahl et al. equation to estimate SST for all core samples.

To verify that this procedure can estimate water temperature correctly, we compared alkenone-based SST and the measured temperature in the modern water column at the study site. Monthly mean and annual mean water temperatures at the core location were derived from the NOAA World Ocean Atlas 1998 (Fig. 4). The estimated $U_{37}^{K'}$-SST (23.2 °C) at the top of the sediment is about 2 °C higher than the annual mean temperature at 0 m depth, but matches the July to October water temperature, suggesting that the estimated SST mainly reflects the temperature of surface water (shallower than 40 m), in summer.

The $U_{37}^{K'}$ values in the piston core sediments vary between 0.60 and 0.83 for the whole core (Table 1). Using these values, SSTs were estimated as between 16.5 and 23.2 °C during the last 130 kyr (Fig. 2g). The maximum $U_{37}^{K'}$ temperature was recorded in the Holocene,

and the minimum value was in MIS 4. The inferred temperature was 17.5 °C at the LGM, i.e., 5.8 °C colder than in the Holocene. This is slightly different than earlier SST estimates at nearby location for February (4 °C) using a transfer function based on planktonic foraminifera (Thompson, 1981).

4. Discussion

4.1. Marine and terrigenous organic carbon estimates

TOC MAR seems to increase synchronously with increases of the C_{37} alkenones and C_{23}–C_{33} *n*-alkanes MARs in the LGM (Fig. 2). It is likely that the major component of TOC is produced by marine plankton; however, we attempted to estimate the proportion of terrigenous organic carbon likely delivered with the *n*-alkanes. Villanueva et al. (1997) developed a mass balance model using two biomarker types, the alkenones and *n*-alkanes, as representative parameters for marine and terrigenous organic matter, respectively. Here we
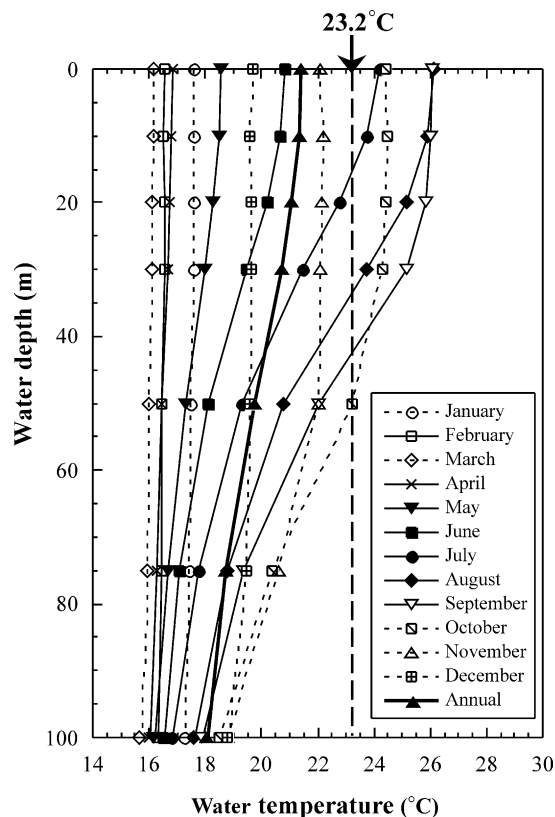
Fig. 4. The profile of monthly and annual mean temperature of the upper 100 m of the water column (World Ocean Atlas, 1998) at the core location. The arrow and dotted line at 23.2 °C indicates SST based on the $U_{37}^{K'}$ of the core top sediment.

take two approaches to verify this estimate; first, we apply Villanueva et al.'s method using biomarker mass balance, and second we compare the results with estimates based on a carbon isotope mass balance model.

Villanueva et al.'s method: The alkenones concentrations are used as an indicator of marine organic matter, and the *n*-alkanes are used as a terrestrial indicator. Assuming that marine organic carbon (C_{marine}) and terrigenous organic carbon ($C_{terrigenous}$) are linearly related to the biomarker concentrations (µg/gdw),

$$C_{marine} = K_m \times [\text{Alkenones}] \qquad (3)$$

and

$$C_{terrigeneous} = K_t \times [\text{Alkanes}] \qquad (4)$$

TOC concentration (µg/gdw) is expressed as:

$$\text{TOC} = K_m \times [\text{Alkenones}] + K_t \times [\text{Alkanes}] \qquad (5)$$

where [Alkenones] is the sum of the $C_{37:2}$ and $C_{37:3}$ alkenone concentrations. [Alkanes] is defined, after Villanueva et al. (1997), as the concentration of odd C_{23}–C_{33} *n*-alkanes. We regarded the area above the line in Fig. 3 as representing the amount of odd C_{23}–C_{33} *n*-alkanes as defined by Villanueva et al. (1997).

Villanueva et al. (1997) assumed that K_m and K_t remain constant in the whole core, and estimated them using all data sets, including the core surface layer. However, we excluded the top 12 cm of the core from further calculations for the following reason. Rapid degradation of organic matter generally occurs at the water–sediment interface and in the near-surface layer of sediments (Emerson et al., 1985). Such early diagenesis takes place at the surface layer of most pelagic sediments. Underlying layers of the core also suffer from degradation, but are usually relatively stable over a long period (Emerson et al., 1987). Such differences in degradation rates might allow selective preservation of organic components between the uppermost layer and the underlying layers. We concluded that sediments in the upper 12 cm are still undergoing rapid early diagensis, judging from their core description and the chemical condition. The color of the uppermost 12 cm is olive brown, in contrast to the olive gray color of the underlying layer. This corresponds to the result that Mn concentration has been reported to be significantly higher (0.17–0.24%) in the upper 12 cm of sediment than in the underlying horizons (0.01–0.06%) of the same core (Murayama and Hayashi, personal communication), indicating oxic conditions in the upper 12 cm of sediment. We concluded that K_m and K_t values in this interval might not be consistent with values in deeper layers, because long-chain alkenones and *n*-alkanes should be more resistant than the early diagenetic organic assemblage indicated by the TOC values of the uppermost 12 cm. Consequently the ratio of biomarkers:TOC should vary in the uppermost layer.

Because we aimed to reconstruct the sedimentation record of biomarkers over as long a period as possible, we estimated K_m and K_t using data from sediments deeper than 12 cm, and assumed that K_m and K_t were constant over the whole study period, in this core essentially corresponding to the interval from MIS 2 to MIS 5.

We solved for K_m and K_t by multiple-regression analysis as described by Villanueva et al. (1997), using as data points the samples ($n = 29$) that had been analyzed between MIS 2 and 5, with the mass balance equation of (5) for each layer. Our most-likely relation is expressed by

$$\text{TOC} = 2614 \times [\text{Alkenones}] + 421 \times [\text{Alkanes}] \qquad (6)$$

The resulting K_m and K_t seem to differ significantly from Villanueva et al.'s values from North Atlantic cores. Villanueva et al. reported K_m and K_t for two piston cores to be 1639 and 2547, respectively, at SU90/08 (43°30′N, 30°24′W, water depth: 3100 m), and 5624 and 3859, respectively, at SU90/39 (52°34′N, 21°06′W, water depth: 3900 m). Differences may perhaps be ascribed to sedimentary conditions such as phytoplankton assemblages in the water column and the specific source of terrestrial organic matter. For example, the terrestrial fraction in the Atlantic SU90/08 core is composed mainly of ice-transported organic matter, whereas the terrestrial organic matter in Shatsky Rise core S-2 was supplied mainly by eolian dusts. Such differences of origin may cause a difference of *n*-alkanes content in the terrestrial organic matter and consequently change the ratio of *n*-alkanes to the sedimentary TOC.

Eq. (6) can be used to reconstruct the TOC profiles using the biomarker concentrations. Fig. 5 shows a comparison between estimated TOC and the observed results in the core. As explained before, we excluded the Holocene data (the surface 12 cm layer) when estimating K_m and K_t. However, to evaluate such an effect, we also plotted the Holocene estimates, using the same relation. The estimated TOC gave values consistent with measured values (Fig. 5) for the period from MIS 2 to MIS 5. The correlation factor between both sets of data was obtained as $r = 0.92$ ($n = 29$). On the other hand, the estimated TOC values in the Holocene were significantly smaller than the observed results. We presume that the observed TOC includes excess carbon from decomposable organic matter, which may not be represented by resistant biomarkers and is lost during early diagenesis. Similar results can be seen in North Atlantic core SU90/08 (Fig. 9 in Villanueva et al., 1997), but the effect was ignored, probably because only limited Holocene samples were taken in the Atlantic core.

Our analysis was also confirmed by a comparison with another proxy for organic matter. We applied an isotope mass balance model using $\delta^{13}C$ of organic mat-
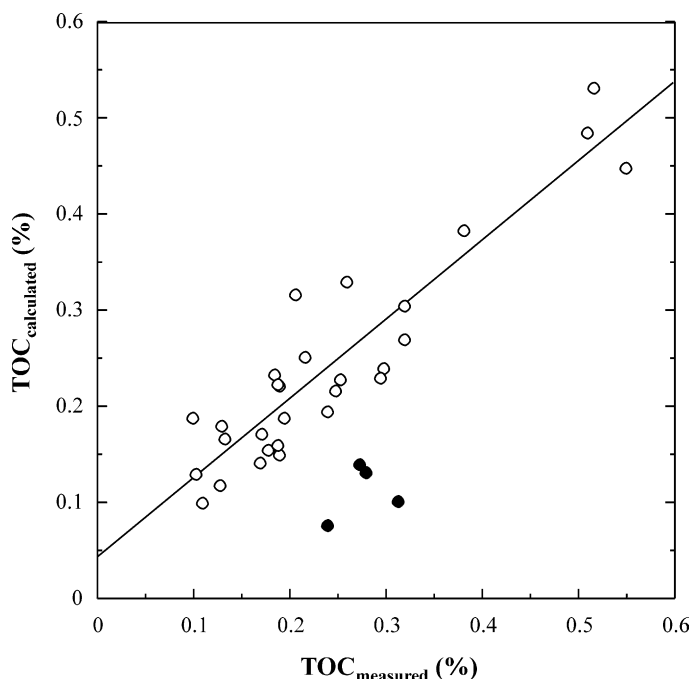
Fig. 5. Correlation plot of the calculated TOC (TOC$_{calculated}$) and the measured TOC (TOC$_{measured}$). Solid circles are the samples in Holocene, and open circles are those in MIS 2–5. The regression line (TOC$_{calculated}$ = 0.83×TOC$_{measured}$ + 0.04) excludes the Holocene samples (solid circles).

ter for comparison. This has conventionally been used to estimate the proportion of marine and terrigenous organic carbon from $\delta^{13}C$ of TOC for Quaternary marine sediments (e.g., Rühlemann et al., 1996).

The $\delta^{13}C$ of the sedimentary bulk organic carbon ($\delta^{13}C_{bulk}$) is expressed as;

$$\delta^{13}C_{bulk} = f_{marine} \times \delta^{13}C_{marine}$$

$$+ f_{terrigenous} \times \delta^{13}C_{terrigenous} \quad (7)$$

$$f_{terrigenous} = 1 - f_{marine} \quad (8)$$

$$C_{marine} = f_{marine} \times TOC \quad (9)$$

$$C_{terrigenous} = f_{terrigenous} \times TOC \quad (10)$$

where f_{marine} and $f_{terrigenous}$ are the proportions of marine and terrigenous sources, respectively, and $\delta^{13}C_{marine}$, $\delta^{13}C_{terrigenous}$ indicate $\delta^{13}C$ of marine organic carbon and $\delta^{13}C$ of terrigenous organic carbon, respectively. The $\delta^{13}C$ end-member values of marine organic matter in low and middle latitudes are between −21.5 and −17.5‰ with an average of −20‰, and those of terrigenous organic matter derived from vascular C_3 plants are between −29.3 and −25.5‰, with an average of −27‰ (Tyson, 1995). Assuming that the appropriate marine and terrigenous end-members are −20 and −27‰,

respectively, we estimated C_{marine} and $C_{terrigenous}$ concentrations in the sediment. The results compare well with estimates from biomarker concentrations using Eqs. (3) and (4) (Fig. 6). Marine and terrigenous organic carbon estimated from the $\delta^{13}C$ mass balance model shows similar carbon content to the estimate from biomarker concentrations, except for the Holocene (Fig. 6). Both estimates indicate that C_{marine} (> 86% of TOC) is higher than $C_{terrigenous}$ in the whole core. The profiles spanning MIS 2–5 agree well with each other, confirming that our assumptions on K_m and K_t are reasonable for reconstructing marine and terrigenous organic carbon in this interval. On the other hand, in Holocene sediments a discrepancy results between the estimates obtained by different models for C_{marine} (circles in Fig. 6); the C_{marine} estimated by the biomarker model gives lower values than estimates by the $\delta^{13}C$ model. Since the bulk organic matter can reflect both decomposable and resistant organic materials, the estimate from the $\delta^{13}C$ model might reproduce the contribution of decomposable organic matter more faithfully than in the case of biomarker proxies. However, this consideration suggests that it is not appropriate to use the bulk $\delta^{13}C$ model to compare the Holocene sediments with those in MIS 2–5, because the decomposable organic matter would be lost in the early diagenesis. Although alkenone can sometimes be degraded in the water column (Prahl et al., 1993), it can also be preserved in
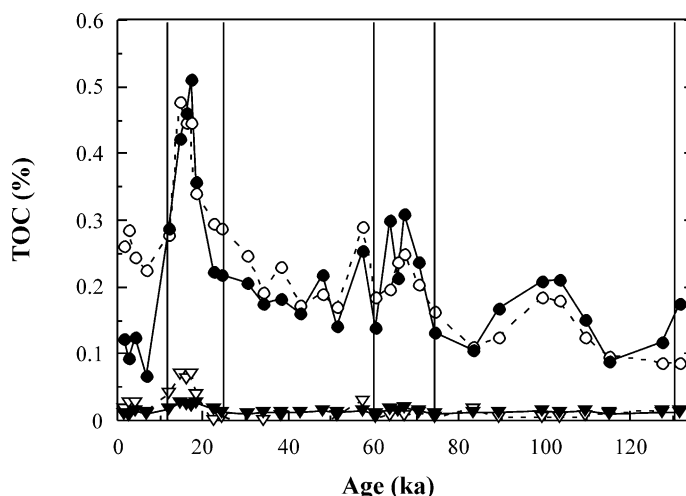
Fig. 6. C_{marine} and $C_{terrigenous}$ estimated from biomarker concentrations and $\delta^{13}C$ of organic matter are plotted against age. C_{marine} estimated from alkenones using Eq. (3) (solid circles with solid line), $C_{terrigenous}$ estimated from *n*-alkanes using Eq. (4) (solid triangles with solid line), C_{marine} estimated from $\delta^{13}C$ using Eq. (9) (open circles with dotted line) and $C_{terrigenous}$ estimated from $\delta^{13}C$ using Eq. (10) (open triangles with dotted line).

sediments for a long time (Farrimond et al., 1986), so it is not clear whether the biomarkers are more stable than the bulk organic matter in the deeper core. In spite of these unknowns, we presume that alkenones can be better indicators of primary production than the bulk organic matter. In addition, the bulk $\delta^{13}C$ model has uncertainty in determining the $\delta^{13}C$ of the end members, especially for marine organic matter. It is known that the carbon isotope discrimination factor in primary production is a function of many environmental factors (Rau et al., 1997). In the glacial-interglacial transition, the $\delta^{13}C$ of marine plankton might have shifted, owing to changes in environmental factors such as atmospheric pCO_2, nutrient concentrations in seawater and surface water temperature. Unfortunately the $\delta^{13}C$ of molecular compounds is not yet available for this site, so it is not clear how the $\delta^{13}C$ of bulk C_{marine} might have varied during this interval. Thus, we conclude that the C_{marine} estimated by the biomarker model gives a more comprehensive comparison for the whole core, although it tends to underestimate the proportion in the upper layer.

4.2. Latitudinal shift of Subarctic front

Fig. 7 shows the temporal trends of the MARs for C_{marine} and $C_{terrigeneous}$ as estimated from biomarker analyses. The C_{marine} increased in glacial times, with the highest values during the LGM and relatively lower values in interglacials (Fig. 7). Biogenic opal MARs are reported to also be higher during the LGM on the Shatsky Rise (Kawahata et al., 1999; Yamane, 2003). These results suggest that marine productivity was higher during the LGM. If plankton productivity was

enhanced in the LGM, then an increase of nutrient concentration in the euphotic zone is needed. One possible cause for such an increase is a southward shift of the Subarctic front. The Subarctic front in the modern North Pacific Ocean is formed around 42°N by the interface of the "Kuroshio" warm current and the "Oyashio" cold current (Fig. 1), and is characterized by high nutrient concentration and low temperature.

A previous study of the shift of the Subarctic front in the western North Pacific was performed using the sinistral coiling of the planktonic foraminifera *Neogloboquadrina pachyderma* (Thompson and Shackleton, 1980). They reported that the Subarctic front might have moved southward to between 35 and 38°N in MIS 2. Our alkenone analyses also showed that $U_{37}^{K'}$-derived SST was 5–6 °C lower at the LGM than at present (Fig. 2g). On the other hand, a previous study on $U_{37}^{K'}$-derived SST for the Kuroshio Current region, the Nishishichitou Ridge off central Japan, showed that SSTs in the LGM were 2–3 °C lower than at present (Sawada and Handa, 1998). The SST estimates at the Shatsky Rise clearly show lower temperatures than for the Kuroshio Current region, which suggests that the SST on the Shatsky Rise was affected not only by a decrease in the SST of the Kuroshio Current itself, but also by the addition of cold surface water, due to the southward shift of the Subarctic front. This confirms the conclusion of Thompson and Shackleton (1980). The lowering of alkenone-derived SST was uninterrupted during the last glacial period (MIS 2–4) suggesting that Subarctic water might have extended over site S-2 throughout the last glacial period.

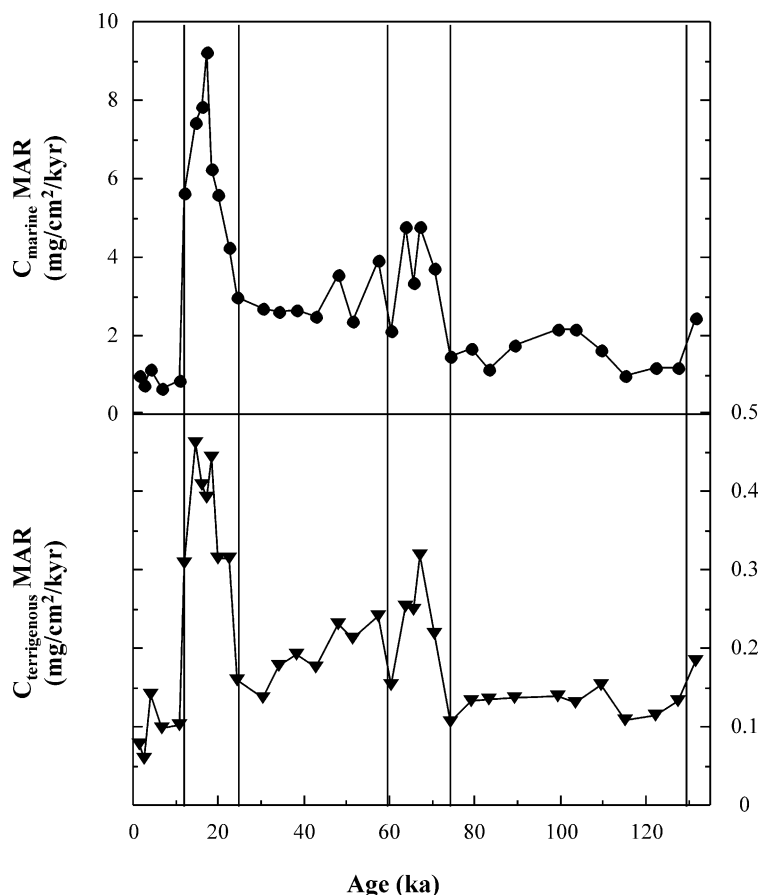Although the interval indicating higher C_{marine} accumulation is roughly consistent with the time of persis-

Fig. 7. Downcore profiles of C_{marine} MAR (mg/cm^2/kyr) and $C_{terrigenous}$ MAR (mg/cm^2/kyr) estimated from biomarker concentration.

tent cold waters (Figs. 2g and 7), it should be noted that C_{marine} MAR was markedly higher only in the LGM and not during MIS 3 and 4. If the southward shift of the Subarctic front was the only factor to control marine productivity, then C_{marine} MAR should be high throughout the glacial period. It seems, therefore, that biological production was stimulated by additional factors during the LGM. According to the most recent study of the Shatsky Rise (Maeda et al., 2002), the primary productivity (PP) based on TOC, biogenic opal/carbonate ratios and the $C_{organic}/C_{carbonate}$ ratios during the last 180 kyr have been higher in the northern domain (core NGC108 at 36°N) of the Shatsky Rise, compared with the southern domain S2612 (32°N). Thus, the authors concluded that the surface water at 36°N has been influenced by Subarctic water mass more than at 32°N, which has been more affected by Subtopical water. The C_{marine} MAR of our study site S-2 (33°N) also shows similar values to the reported TOC MAR at 32°N rather than that at 36°N; we therefore presume that the Subarctic front did not reach 33°N, even in the LGM. This conclusion must be verified by

further studies of water mass movement; however there are no other indications in core S-2 to support the existence of Subarctic water. For instance, no obvious change has been found in $\delta^{15}N$ of TN (total nitrate) throughout the core, indicating that nitrate concentration in the mixed layer did not vary significantly over this site. Hence, our results of SST and C_{marine} MAR suggest that the enhancement of productivity in the LGM could not have been caused only by the southward shift of the Subarctic front, but must have involved additional factors.

4.3. Eolian dust input

Fig. 7 shows that $C_{terrigeneous}$ accumulated more than twice as much in MIS 2 as in MIS 3. Such a temporal increase of terrigenous input might be a possible cause of higher primary production; trace nutrients in the terrestrial fraction have been regarded as a limiting factor for phytoplankton growth (Martin and Fitzwater, 1988). The terrigenous material would have to be transported to this core site by atmospheric deposition,

because no river could supply this remote seabed rise. In fact, Murayama et al. (1998) studied metallic elements (Al, Fe, and Ti) in this same core, and concluded that the eolian dust flux was maximal in the LGM, based on the temporal increase of the Al and Ti accumulation rates at this site. The increase of eolian dust deposition during the LGM has been identified as a global event, consistent with a Greenland ice core (GRIP Members, 1993). However, we believe that the lipid biomarkers in our sediment core may mainly reflect dust components that originated from relatively close land areas, such as the Chinese Loess Plateau, rather than dust particles distributed globally in the troposphere. The conversion factor ($K_t = 421$) of n-alkanes for terrigenous carbon is noticeably smaller than the value ($K_t = 2547$ or 3859) estimated in the North Atlantic by Villanueva et al. (1997), suggesting that the proportion of n-alkanes to the dust as a host substance might be larger on the Shatsky Rise. The n-alkanes in the North Atlantic sites were reported to have been delivered from ice-transported materials in which organic matter had already been degraded. Compared with such organic materials, it is likely that the terrigenous organic matter delivered to the Shatsky Rise might have been less degraded and that the land source area might have been closer to the site. In addition, n-alkane distributions show n-C_{31} alkane predominance in the whole core. It is reported that n-C_{31} alkane originates from grassy vegetation (Cranwell, 1973); the high n-C_{31} alkane concentration in our study may result from a grassland/steppe environment, and provides evidence of derivation from the Chinese Loess Plateau. Based on these considerations, we conclude that the most likely source of terrigenous matter during the LGM is eolian dust, mainly from the Chinese continental landmass.

Martin (1990) hypothesized that new production in the modern Southern Ocean is limited by iron deficiency, and that eolian input of iron via dust would have enhanced marine production in the LGM. Recently, it has been shown that several high-nutrient low-chlorophyll (HNLC) areas exist in the North and Central Pacific, where iron can play a similar limiting role. Although it is not clear whether the region near the Shatsky Rise experienced such iron limitation in the glacial period, it is worthwhile examining whether the increase of eolian dust could have enhanced primary production. Chinese Loess and simulated Asian mineral dust are reported to have about 3% iron content (Nishikawa et al., 2000). Although the solubility of iron from such dust particles in seawater has not been reported in detail, it is probable that less than 50% is soluble (Duce et al., 1991) and could supply Fe to seawater. In fact, at one of the HNLC areas near station PAPA (50°N, 145°W) in the eastern North Pacific, it has been reported that the passage of Asian dust storms results in rapid increases of carbon biomass in the mixed layer

(Bishop et al., 2002). Atmospheric iron flux to the area near the Shatsky Rise in the western North Pacific is apparently higher than at station PAPA in the eastern North Pacific (Duce and Tindale, 1991), and consequently could supply iron and other micronutrients to the Shatsky Rise. These indirect lines of evidence support the hypothesis that Asian dust storms might have supplied iron and other micronutrients and thereby enhanced marine productivity during the last glacial period. If this presumption is the case for our study area, then we have to infer surface water conditions similar to the modern HNLC areas. Further study must be done to confirm this inference. Even if nutrients were supplied to the euphotic zone by the southward shift of the Subarctic front, iron input might still have enhanced planktonic production. Furthermore, other nutrients in dust, such as Si and P, might also have enhanced marine production. The eolian dust input clearly played an important role in controlling productivity in the middle latitudes of the western North Pacific. Thus, we emphasize that the role of eolian dust in oligotrophic seas should be reevaluated in detail.

5. Conclusions

We estimated temporal changes during the last 130 kyr of organic carbon fluxes from marine and terrigenous sources in the sediment at the Shatsky Rise. The marine and terrigenous organic carbon accumulations estimated from two biomarker fractions, the alkenones and the n-alkanes, gave estimates consistent with those from $\delta^{13}C$ of TOC in the sediment core, except for samples in the uppermost oxic layer. The C_{marine} was estimated to be more than 86% of the TOC over the whole core. The C_{marine} MAR showed the highest value of 9.2 mgC/cm^2/kyr in the LGM, and relatively high accumulations in glacial periods. We estimate that such higher accumulation rates resulted from efficient biological production, which might have been enhanced by increases of eolian dust supply from China, especially in the LGM. The southward movement of the Subarctic front also enhanced biological activity, but it could not have been the main cause of the enhancement in the LGM, because the alkenone-derived temperature indicates that cold water remained over the site throughout MIS 2–4.

Acknowledgements

Associate Editor—**A. Bishop**

References

Bray, E.E., Evans, E.D., 1961. Distribution of *n*-paraffins as a clue to recognition of source beds. Geochimica Cosmochimica Acta 22, 2–15.

Bishop, J.K.B., Davis, R.E., Sherman, J.T., 2002. Robotic observations of dust storm enhancement of carbon biomass in the North Pacific. Science 298, 817–821.

Collister, J.W., Rieley, G., Stern, B., Eglinton, G., Fry, B., 1994. Compound-specific $\delta^{13}C$ analyses of leaf lipids from plants with differing carbon dioxide metabolisms. Organic Geochemistry 21, 619–627.

Cranwell, P.A., 1973. Chain-length distribution of *n*-alkanes from lake sediments in relation to post-glacial environmental change. Freshwater Biology 3, 259–265.

Duce, R.A., Liss, P.S., Merrill, J.T., Atlas, E.L., Menard, P.-B., Hicks, B.B., Miller, J.M., Prospero, J.M., Arimoto, R., Church, T.M., Ellis, W., Galloway, J.N., Hansen, L., Jickells, T.D., Knap, A.H., Reinhardt, K.H., Schneider, B., Soudine, A., Tokos, J.J., Tsunogai, S., Wollast, R., Zhou, M., 1991. The atmospheric input of trace species to the world ocean. Global Biogeochemical Cycles 5, 193–259.

Duce, R.A., Tindale, N.W., 1991. Atmospheric transport of iron and its deposition in the ocean. Limnology and Oceanography 36, 1715–1726.

Eglinton, G., Hamilton, R.J., 1967. Leaf epicuticular waxes. Science 156, 1322–1335.

Emerson, S., Fischer, K., Reimers, C., Heggie, D., 1985. Organic carbon dynamics and preservation in deep-sea sediments. Deep-Sea Research 32, 1–21.

Emerson, S., Stump, C., Grootes, P.M., Stuiver, M., Farwell, G.W., Schmidt, F.H., 1987. Estimates of degradable organic carbon in deep-sea surface sediments from ^{14}C concentrations. Nature 329, 51–54.

Farrimond, P., Eglinton, G., Brassell, S.C., 1986. Alkenones in Cretaceous black shales, Blake–Bahama Basin, western North Atlantic. Organic Geochemistry 10, 897–903.

Gagosian, R.B., Peltzer, E.T., 1986. The importance of atmospheric input of terrestrial organic material to deep sea sediments. Organic Geochemistry 10, 661–669.

Goericke, R., Fry, B., 1994. Variations of marine plankton $\delta^{13}C$ with latitude, temperature, and dissolved CO_2 in the world ocean. Global Biogeochemical Cycles 8, 85–90.

Greenland Ice-core Project (GRIP) Members, 1993. Climate instability during the last interglacial period recorded in the GRIP ice core. Nature 364, 203–207.

Hovan, S.A., Rea, D.K., 1991. Late Pleistocene continental climate and oceanic variability recorded in Northwest Pacific sediments. Paleoceanography 6, 349–370.

Jasper, J.P., Gagosian, R.B., 1993. The relationship between sedimentary organic carbon isotopic composition and organic biomarker compound concentration. Geochimica Cosmochimica Acta 57, 167–186.

Kawahata, H., Ohkushi, K., Hatakeyama, Y., 1999. Comparative Late Pleistocene paleoceanographic changes in the mid latitude boreal and austral western Pacific. Journal of Oceanography 55, 747–761.

Kawahata, H., Okamoto, T., Matsumoto, E., Ujiie, H., 2000. Fluctuations of eolian flux and ocean productivity in the mid-latitude North Pacific during the last 200 kyr. Quaternary Science Reviews 19, 1279–1291.

Maeda, L., Kawahata, H., Nohara, M., 2002. Fluctuation of biogenic and abiogenic sedimentation on the Shatsky Rise in the western North Pacific during the late Quaternary. Marine Geology 189, 197–214.

Marlowe, I.T., Brassell, S.C., Eglinton, G., Green, J.C., 1984. Long chain unsaturated ketones and esters in living algae and marine sediments. Organic Geochemistry 6, 135–141.

Martin, J.H., 1990. Glacial-interglacial CO_2 change: The iron hypothesis. Paleoceanography 5, 1–13.

Martin, J.H., Fitzwater, S.E., 1988. Iron deficiency limits phytoplankton growth in the north-east Pacific subarctic. Nature 331, 341–343.

Murayama, M., Hayashi, K., Yamane, M., Narita, H., Oba, T., 1998. Terrigenous input and ^{10}Be flux records from the Shatsky Rise; implications for land-ocean linkages in the Northwest Pacific. In: Program and Abstracts of 6th International Conference on Paleoceanography, pp. 170–171.

Nishikawa, M., Hao, Q., Morita, M., 2000. Preparation and evaluation of Certified Reference Materials for Asian mineral dust. Global Environmental Research 4, 103–113.

Prahl, F.G., Muehlhausen, L.A., Lyle, M., 1989. An organic geochemical assessment of oceanographic conditions at MANOP site C over the past 26,000 years. Paleoceanography 4, 495–510.

Prahl, F.G., Muehlhausen, L.A., Zahnle, D.L., 1988. Further evaluation of long-chain alkenones as indicators of paleoceanographic conditions. Geochimica Cosmochimica Acta 52, 2303–2310.

Prahl, F.G., Collier, R.B., Dymond, J., Lyle, M., Sparrow, M.A., 1993. A biomarker perspective on prymnesiophyte productivity in the northeast Pacific Ocean. Deep-Sea Research I 40, 2061–2076.

Rau, G.H., Riebesell, U., Wolf-Gladrow, D., 1997. CO_{2aq}-dependent photosynthetic ^{13}C fractionation in the ocean: a model versus measurements. Global Biogeochemical Cycles 11, 267–278.

Rostek, F., Bard, E., Beaufort, L., Sonzogni, C., Ganssen, G., 1997. Sea surface temperature and productivity records for the past 240 kyr in the Arabian Sea. Deep-Sea Research II 44, 1461–1480.

Rühlemann, C., Frank, M., Hale, W., Mangini, A., Mulitza, S., Müller, P.J., Wefer, G., 1996. Late Quaternary productivity changes in the western equatorial Atlantic: evidence from

230Th-normalized carbonate and organic carbon accumulation rates. Marine Geology 135, 127–152.

Sarnthein, M., Winn, K., Duplessy, J.-C., Fontugne, M.R., 1988. Global variations of surface ocean productivity in low and mid latitudes: influence on CO_2 reservoirs of the deep ocean and atmosphere during the last 21,000 years. Paleoceanography 3, 361–399.

Sawada, K., Handa, N., 1998. Variability of the path of the Kuroshio ocean current over the past 25,000 years. Nature 392, 592–595.

Sicre, M.-A., Ternois, Y., Paterne, M., Boireau, A., Beaufort, L., Martinez, P., Bertrand, P., 2000. Biomarker stratigraphic records over the last 150 kyears off the NW African coast at 25°N. Organic Geochemistry 31, 577–588.

Simoneit, B.R.T., 1977. Organic matter in eolian dusts over the Atlantic Ocean. Marine Chemistry 5, 443–464.

Thompson, P.R., 1981. Planktonic foraminifera in the western North Pacific during the past 150,000 years: comparison of modern and fossil assemblages. Palaeogeography Palaeoclimatology Palaeoecology 35, 241–279.

Thompson, P.R., Shackleton, N.J., 1980. North Pacific palaeoceanography: late Quaternary coiling variations of planktonic foraminifer *Neogloboquadrina pachyderma*. Nature 287, 829–833.

Tyson, R.V., 1995. Sedimentary Organic Matter: Organic Facies and Palynofacies. Chapman and Hall, London.

Villanueva, J., Grimalt, J.O., Cortijo, E., Vidal, L., Labeyrie, L., 1997. A biomarker approach to the organic matter deposited in the North Atlantic during the last climatic cycle. Geochimica Cosmochimica Acta 61, 4633–4646.

Villanueva, J., Grimalt, J.O., Labeyrie, L.D., Cortijo, E., Vidal, L., Turon, J.-L., 1998. Precessional forcing of productivity in the North Atlantic Ocean. Paleoceanography 13, 561–571.

Volkman, J.K., Eglinton, G., Corner, E.D.S., Sargent, J.R., 1980. Novel unsaturated straight-chain C_{37}-C_{39} methyl and ethyl ketones in marine sediments and a coccolithophore *Emiliania huxleyi*. In: Douglas, A.G., Maxwell, J.R. (Eds.), Advances in Organic Geochemistry 1979. Pergamon, Oxford, pp. 219–227.

World Ocean Atlas, 1998. NOAA, National Oceanographic Data Center, Ocean Climate Laboratory, April 1999.

Yamane, M., 2003. Late Quaternary variations in water mass in the Shatsky Rise area, northwest Pacific Ocean. Marine Micropaleontology 48, 205–223.